Journal of Chromatography, 544 (1991) 345–370
Elsevier Science Publishers B.V., Amsterdam

CHROM. 23 188

Review

Characterization of bonded phases by solid-state NMR spectroscopy

KLAUS ALBERT and ERNST BAYER*
Institut für Organische Chemie, Auf der Morgenstelle 18, W-7400 Tübingen (Germany)

ABSTRACT

Structure and dynamics of chemically modified silica gels have been investigated by high-resolution solid-state NMR spectroscopy. ^{29}Si cross-polarization–magic angle spinning (CP–MAS) NMR spectroscopy yields information on variety and quantity of surface species of both pure silica gel and modified silica gel. ^{13}C CP–MAS NMR spectroscopy reveals dynamic properties of the attached alkyl chains. The data from ^{29}Si and ^{13}C solid-state NMR spectroscopy can be correlated with the separation characteristics in high-performance liquid chromatography.

CONTENTS

1. INTRODUCTION

Despite the wide use of bonded phases in high-performance liquid chromatography (HPLC), little is known about the structural and dynamic behaviour of these important materials. In modern HPLC most separations are performed in the re-

0021-9673/91/$03.50

versed-phase mode using chemically modified silica and/or polymer packing materials as stationary phases [1,2]. This paper deals with the characterization of chemically modified silica gels, which are still widely employed in practical HPLC. In a further review, the structural and dynamic behaviour of polymer packing materials will be discussed.

Valuable structural information about the basic gel and the chemically modified material can be obtained with the help of solid-state NMR spectroscopy. To improve the understanding of this NMR measuring technique, the detection principle and relaxation time measurement sequences are first outlined. Surface characterization of pure silica gel is then described, and succeeding sections deal with structural and dynamic investigations of modified materials.

2. HIGH-RESOLUTION SOLID-STATE NMR AND RELAXATION TIME MEASUREMENTS

NMR spectra of solid material measured with the routine equipment for solution NMR would only result in extremely broad lines covering the whole range of the NMR spectrum. This phenomenon is due to the direct neighbourhood of atoms in the lattice causing strong dipolar-dipolar and chemical shift anisotropy interactions. Fortunately, the tensor-like behaviour of both types of interaction is dependent on the orientation θ to the external magnetic field and strongly relates to $3\cos^2\theta - 1$. Therefore, line broadening effects due to dipolar and chemical shift anisotropy effects can be cancelled if the term $3\cos^2\theta - 1$ is set to zero, resulting in a "magic angle" of 54.7° to the external magnetic field. Rotating a sample at this angle (magic angle spinning, MAS [3]) with a rotation speed (3000–4000 Hz) higher then the frequency range of interactions will cause a collapse of disturbances and result in narrow NMR line widths. Two further problems arise in solid-state NMR spectroscopy, one related to strong heteronuclear interactions being present and the other to the existence of very long spin–lattice relaxation times T_1 of the order of minutes to hours. The problem of strong heteronuclear interactions can be solved by high-power decoupling [4] using a proton decoupler with a power of up to 1000 W.

The spin–lattice relaxation time T_1 of a nucleus determines the pulse repetition rate in an NMR experiment. If the T_1 values are in the range of hours, the application of MAS for the investigation of reversed phases is very unfavourable. The problem of long relaxation times can be overcome by the cross-polarization (CP) concept of Pines *et al.* [5]. Here, a "dilute" nucleus such as ^{13}C or ^{29}Si in a ^{1}H lattice is excited in a double-resonance experiment via the surrounding protons. In the measuring sequence (Fig. 1, outlined for ^{13}C nuclei) a proton 90° pulse first builds up proton transverse magnetization. Owing to a 90° phase shift in the ^{1}H radiofrequency (r.f.) field (H_{1H}), the proton magnetization is maintained in a "spin-lock" condition in which proton spin polarization is transferred to ^{13}C spin polarization. At the beginning of the spin-lock condition a ^{13}C r.f. field H_{1C} is applied under conditions of the Hartmann–Hahn match $\gamma_H H_{1H} = \gamma_C H_{1C}$. The build-up of ^{13}C magnetization is performed in a distinct contact period, in which the energy levels of the abundant ^{1}H and rare ^{13}C spins are the same. After the contact period the ^{13}C r.f. is turned off, whereas the proton r.f. field is maintained for spin-locking conditions and for ^{1}H decoupling. After a relaxation delay which is now only dependent on the ^{1}H spin–lattice relaxation time, the whole double resonance experiment can be repeated. Because only ^{13}C

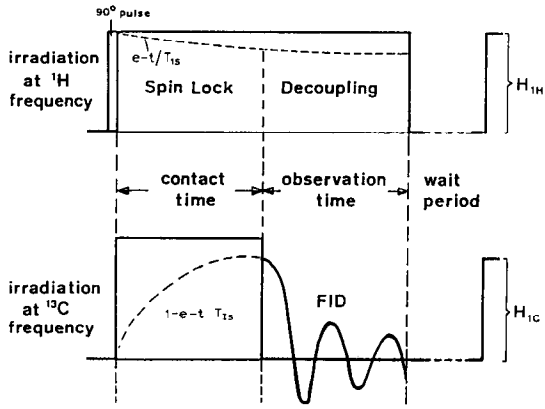

Fig. 1. Cross-polarization timing diagram.

and ^{29}Si nuclei, which are in close contact with protons (no more than four bonds away), are polarized, the combined CP–MAS measuring sequence is the method of choice for the investigation of bonded phases because of its surface selectivity.

The build-up of ^{13}C or ^{29}Si magnetization proceeds at a rate determined by the cross-relaxation constants T_{CH} and T_{SiH}, respectively. The fall-off of ^{13}C or ^{29}Si magnetization is due to the decrease in the spin-locked ^{1}H magnetization which decays with the proton spin–lattice relaxation time in the rotating frame $T_{1\rho H}$.

Contact-time variation experiments give the dependence of the amplitude of the ^{13}C or ^{29}Si signal on the applied contact time (as an example, see Fig. 3, showing the behaviour of the ^{29}Si CP–MAS amplitude of the signals of basic silica gel as a function of contact time). Such a series of spectra is useful for determining T_{CH} (T_{SiH}) and $T_{1\rho H}$.

In the suspended state, the determination of spin–lattice relaxation time T_1 proved to be a valuable tool for deriving information about the dynamic behaviour of alkyl-modified silica. In this type of measurement, a 180° pulse inverts the M_z magnetization. After a variable delay τ, the residual magnetization is detected by a 90° pulse. Depending on the length of τ, the signal intensity may be negative (inverted), zero (no absorption) or positive (absorption). T_1 can be calculated either by taking the zero transition state τ_0 (the case of no absorption) as a crude measure ($T_1 = \tau_0 \ln 2$) or by a least-squares fit of all data of the inversion–recovery curve.

These measurements give information on motions in the range of Larmor frequencies, *e.g.*, the MHz regime. Owing to the application of the spin lock in the cross-polarization experiment, the kHz motional regime is open for investigation. Thus, by combination of both types of experiments, information about the dynamic behaviour of a system in the kHz and MHz ranges can be derived.

Spin–lattice relaxation times in the rotating frame, $T_{1\rho H}$, can be measured directly by inserting a variable relaxation delay τ between the beginning of the spin lock and the beginning of the contact period [6]. The ^{13}C or ^{29}Si intensity at the end of the contact period depends on the length of τ, in which ^{1}H spin–lattice relaxation occurs. Thus, small τ values result in high ^{13}C or ^{29}Si intensities, whereas the ^{13}C or ^{29}Si intensity decreases with increasing τ values (see Fig. 22 in Section 7).

3. ^{29}Si CP–MAS NMR INVESTIGATIONS

^{29}Si chemical shifts are detected over a range of 400 ppm and are well suited to give valuable information on the various structural elements of the silica gel surface. Structural assignments adopted in solution can be used for the interpretation of solid-state ^{29}Si NMR spectra because chemical shifts in the liquid and the solid state differ to only a minor extent [7]. For the presentation of the structure of surface species, a modified notation of Engelhardt *et al.* [7] is adopted, indicating the different types of Q_n, M_n, D_n and T_n units as subscripts.

3.1. Basic silica gel

A typical ^{29}Si CP–MAS NMR spectrum of a silica gel shows three signals: geminal silanol groups Q_2, silanol groups Q_3 and siloxane groups Q_4 are indicated by signals at -91, -100 and -109 ppm [8], respectively (Fig. 2). Thus, ^{29}Si solid-state NMR spectroscopy allows the differentation between free silanol groups and geminal silanol groups, which is not possible by infrared techniques. The drawback of ^{29}Si CP–MAS NMR spectroscopy is the problem of signal quantification. The signal amplitudes of all groups are dependent on the applied contact time (Fig. 3). The CP curves pass through a maximum value. The maximum signal-to-noise ratio for a particular signal is obtained when that corresponding to the maximum on the CP curve is chosen. The resonances of Q_2 and Q_3 exhibit similar amplitude maxima at a contact time of 3–5 ms, whereas the signal of Q_4 shows a broad maximum in the range 10–25 ms. This phenomenon is due to the different relaxation times, T_{SiH} and $T_{1\rho H}$, of Q_2, Q_3 and Q_4. For example, in the case of Nucleosil 100-7 batch 4111 (Fig. 4), the following values are obtained for T_{SiH} and $T_{1\rho H}$, respectively ($T_{1\rho H}$ values are determined at a contact time of 4 ms) [9]: Q_2, 0.9 and 7.4; Q_3, 1.4 and 14.2; and Q_4,

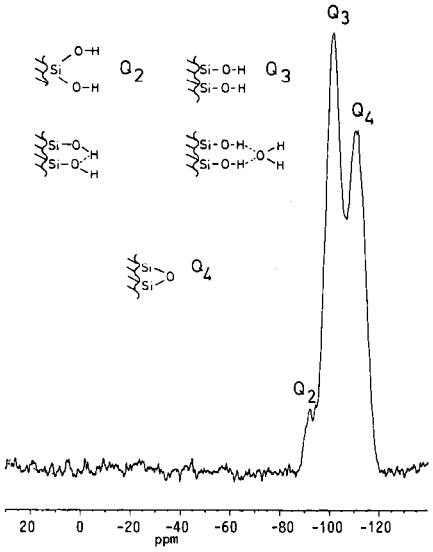

Fig. 2. ^{29}Si CP–MAS NMR spectrum of basic silica gel.

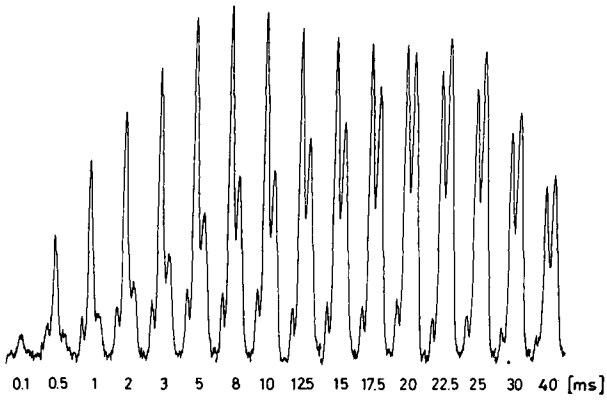

Fig. 3. Behaviour of ^{29}Si CP–MAS amplitude of the signals of basic silica gel as a function of contact time.

4.5 and 15.1 ms. $T_{1\rho H}$ turns out to be considerably larger than T_{SiH}, and therefore the signal amplitudes are determined largely by the T_{SiH} values. In the case of Q_4 groups, the larger T_{SiH} value causes a shift in the CP curve to higher contact times.

With a knowledge of the relaxation times, the Q_2:Q_3:Q_4 ratio of the silica suface can be determined according to the equation [9]

$$I_t = (I_o/T_{SiH})\{[\exp(-t/T_{1\rho H}) - \exp(-t/T_{SiH})]/(1/T_{SiH} - 1/T_{1\rho H})\}$$

Using the above equation, the surface Q_2:Q_3:Q_4 ratio of Nucleosil batch 4111 is 9.3:51.8:38.8. Owing to the surface selectivity of the CP sequence, bulk Q_4 groups are not detected. Inner silanol groups of the silica surface, which are not involved in the chromatographic process, also account for the number of Q_2 and Q_3 groups.

Dynamic studies of the silica surface are not only necessary for quantification purposes but also yield valuable information about the history of surface treatment. Fig. 5 shows the contact curve of Q_2, Q_3 and Q_4 of Nucleosil batch 5061. No signif-

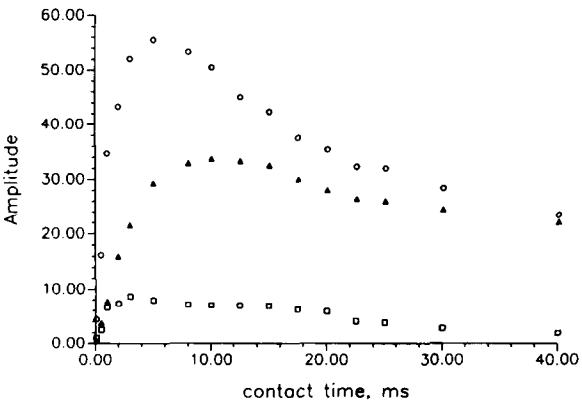

Fig. 4. Cross-polarization curve of (□) Q_2, (○) Q_3 and (▲) Q_4 units of Nucleosil batch 4111.

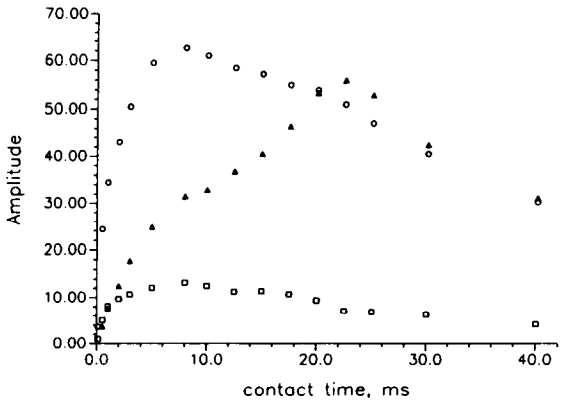

Fig. 5. Cross-polarization curve of (□) Q_2, (○) Q_3 and (▲) Q_4 units of Nucleosil batch 5061.

icant changes are found in the CP curve of Q_2 and Q_3, whereas the signal amplitude behaviour of Q_4 is different with respect to batch 4111. In addition to the broad maximum at 22.5 ms, a second maximum at 8 ms is found. Here two different T_{SiH} values of 1.7 and 21.5 ms can be determined (Fig. 6a) and also two different $T_{1\rho H}$

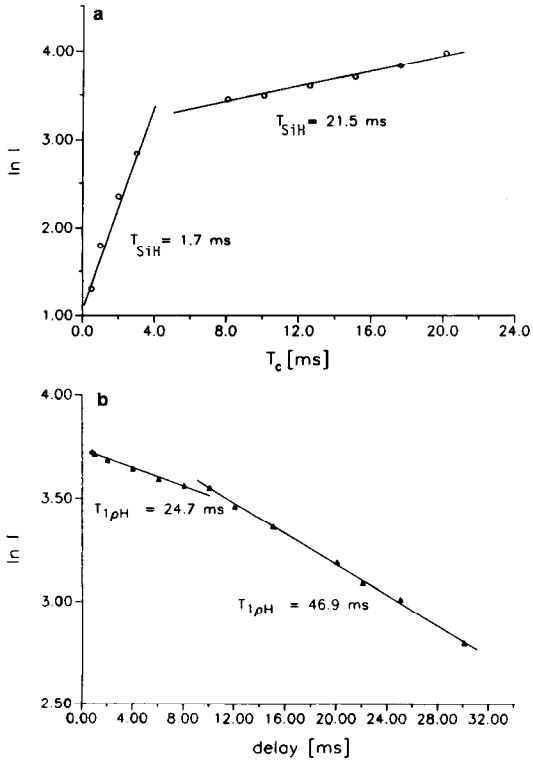

Fig. 6. (a) Development of ^{29}Si magnetization of siloxane units Q_4 of Nucleosil batch 5061 characterized by the time constant for maximum ^{29}Si magnetization, T_{SiH}. (b) Decay of ^{29}Si magnetization of siloxane units Q_4 of Nucleosil batch 5061 characterized by the relaxation time in the rotating frame, $T_{1\rho H}$.

values of 24.7 and 46.9 ms (Fig. 6b). A similar situation prevails for acid-pretreated silica: at least two different regions on the surface of the silica exist: amorphous silica, with relative large T_{SiH} and $T_{1\rho H}$ values, and polycrystalline domains, with small T_{SiH} and $T_{1\rho H}$ values [9,10]. These domains can be ascribed to β-tridymite-like structures, which is further proved by electron diffraction methods [11].

3.2. Chemically modified silica gel

Silica gel is modified with either mono, di- or trifunctional silanes [12–14]. According to the type of silane used, different surface species may result (Fig. 7), and these can be distinguished by ^{29}Si CP–MAS NMR spectroscopy [15–32]. While the M_1 unit is the main product of the reaction with monofunctional silanes, di- and trifunctional silanes yield numerous different surface species (see Fig. 7). In addition to the first modification step, a second treatment is often performed. This "end-capping" with hexamethyldisilazane–trichlorosilane introduces an $Si(CH)_3$ moiety M_2 in order to reduce the number of silanol groups.

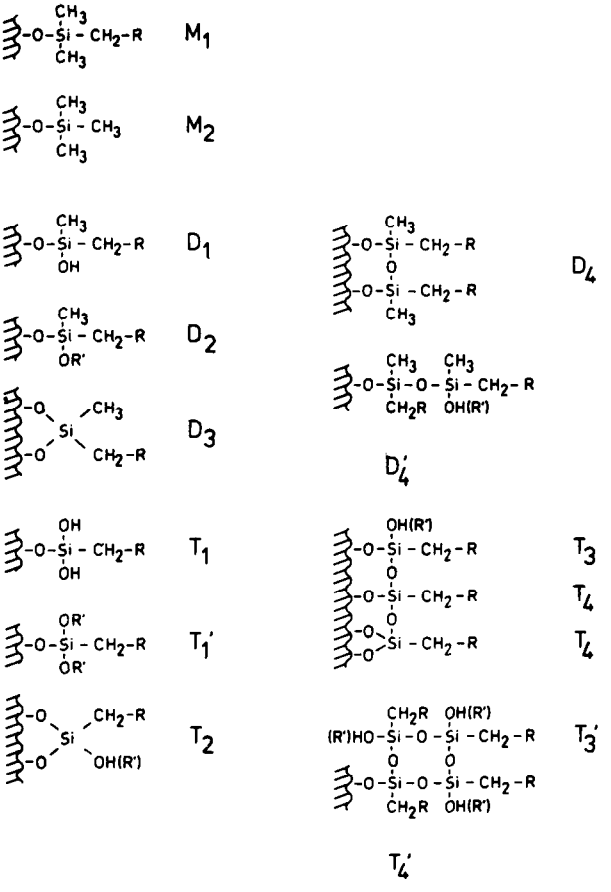

Fig. 7. Surface species of chemically modified silica gels.

3.2.1. Monofunctionally derivatized silica gel. In addition to the signals of bulk silica, Q_2, Q_3 and Q_4, a resonance of the M_1 unit is seen at +12 ppm (Fig. 8). The silane signal itself shows relatively large variation in cross-polarization behaviour with T_{SiH} values varying from 2 to 4 ms and $T_{1\rho H}$ values from 30 to 100 ms [9]. Therefore, the optimum contact times differ by 5–15 ms. The variations follow more or less those of the existing Q_3 and Q_4 signals of the corresponding parent silica. The differences probably reflect different silane mobilities of different silica supports.

3.2.2. Difunctionally derivatized silica gel. Spectra of difunctionally derivatized silica gels show the resonances of the silanes at −4 to −22 ppm in addition to the signals of geminal silanediol groups Q_2, silanol groups Q_3 and siloxane groups Q_4 of the native silica gel. After reaction of silica with octadecylmethyldichlorosilane, for instance, signals of D_1 (−4 ppm), D_2 (−7 ppm), D_3 (−10 ppm) and of various D_4 + D_4' species (−14 to −22 ppm) are obtained [9,28,32].

In contrast to monofunctionally derivatized silica gels, the silane signals of difunctionally modified silica gels show similar cross-polarization behavior with T_{SiH} values of 0.5–0.8 ms and $T_{1\rho H}$ values of 14–31 ms, yielding a contact time maximum of about 5 ms [32]. Therefore, the amounts of various surface species after distinct modification procedures can be determined. Fig. 9 shows the D regions of the ^{29}Si CP–MAS NMR spectra of difunctionally modified Nucleosil prepared under different modification conditions. Derivatization without atmospheric exclusion favours condensation to polymeric species D_4 + D_4' (50%), whereas monodentates D_1 and D_2 and the bidentate D_3 species are formed to 36% and 8%, respectively (Fig. 9a). In addition to the signals already assigned, a signal at +1.6 ppm was found, amounting

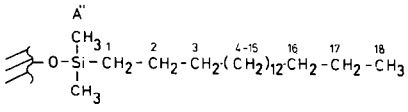

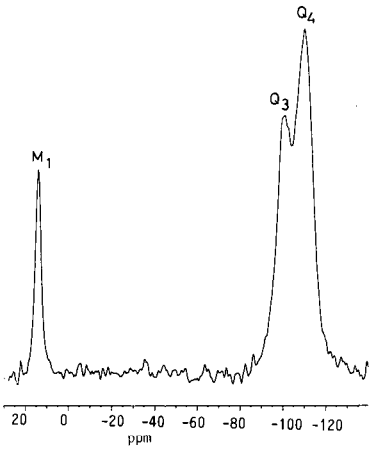

Fig. 8. ^{29}Si CP–MAS NMR spectrum of monofunctionally derivatized silica gel.

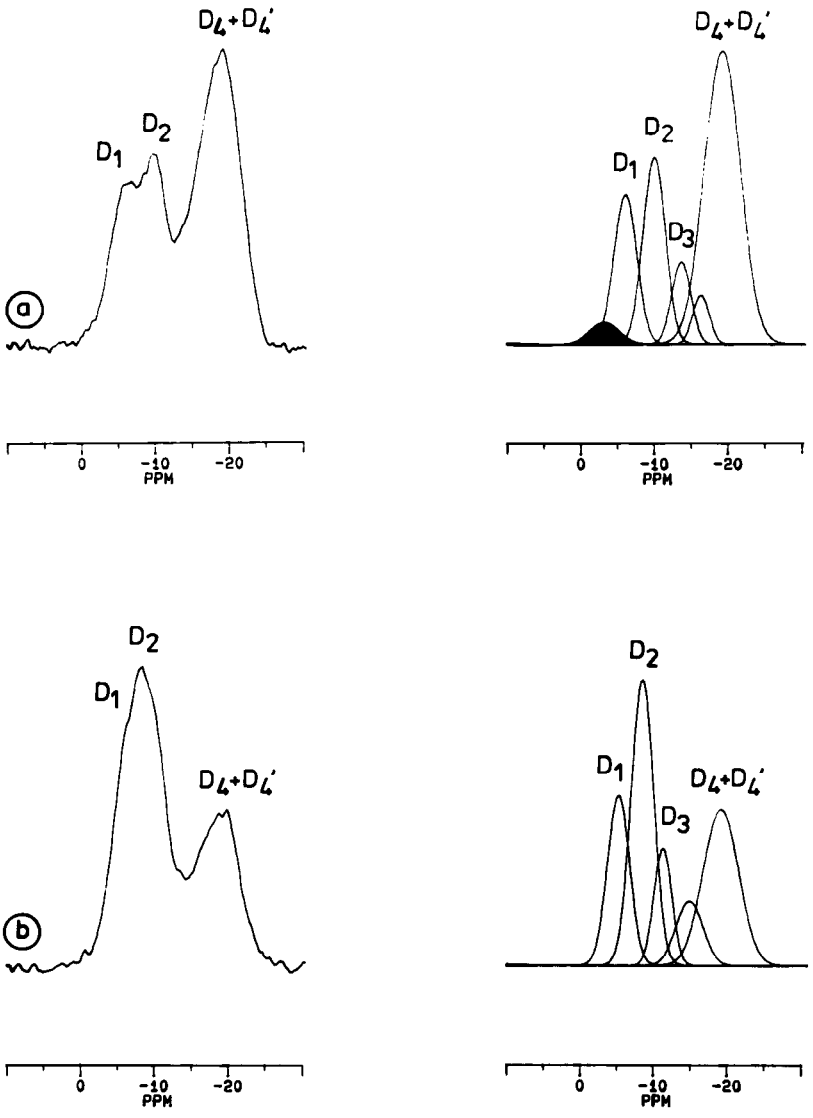

Fig. 9. Comparison of ^{29}Si CP–MAS NMR spectra of difunctionally modified silica gel under experimental (left) and simulated (right) conditions: (a) after silylation in the presence of air; (b) after silylation under an argon atmosphere.

to 3% of the total intensity. This resonance has also been obtained for other difunctionally modified phases.

Modification under an argon atmosphere leads to the preferred formation of monodentates D_1 and D_2 (52%), whereas the amount of bidentate D_3 is 11% and of condensed species D_4 + D_4' 36% (Fig. 9b). In the case of difunctional derivatization with dichlorosilane (Fig. 10), the first step is the formation of the monodentate I. The

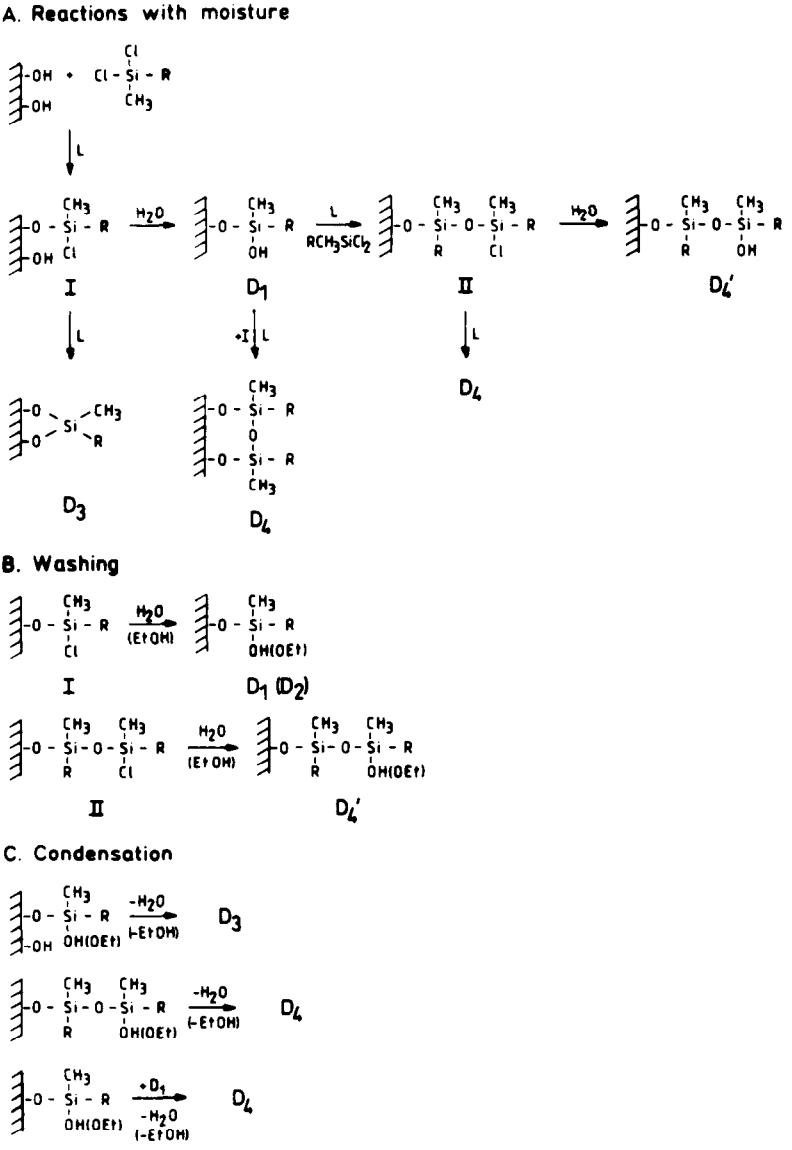

Fig. 10. Reaction scheme for difunctional modification of silica gel. Et = ethyl.

intermediate is hydrolysed during washing at the end of the synthesis to the monodentates D_1 and D_2. Therefore, the amount of D_2 is an indirect indication of the amount of monodentate I at the end of the reaction, as the D_2 species can be formed from I in the washing step with ethanol only. A large amount of D_2 can be correlated with a large amount of monodentate I. Hence, the large amount of D_2 in reactions in an argon atmosphere reveal that many of the monodentate I species neither have formed condensed species nor have reacted with the silica to form bidentate D_3.

However, the small amount of D_3 formed in both the presence and absence of moisture clearly indicates that the bidentate D_3 formation, although not favoured (as seen in Fig. 9), still occurs. The ratio of monodentate (D_1, D_2) to bidentate (D_3) after the washing step always exceeds 3:1. This indicates that the formation of monodentates D_1 and D_2, even in the presence of moisture, is always preferred.

3.2.3. Trifunctionally derivatized silica gel. After reaction of silica gel with octadecyltrichlorosilane, resonances of T_1 (−46 ppm), T_1' (−50 ppm), T_2 (−56 ppm), T_3 + T_3' (−59 ppm) and T_4 + T_4' species (−64 to −70 ppm) result [9, 28, 32]. The optimum contact time for all T units is 2.5 ms, with T_{SiH} values of 0.4–0.7 ms and $T_{1\rho H}$ values of 16–30 ms, independent of the silica gel used [32]. It is interesting that in

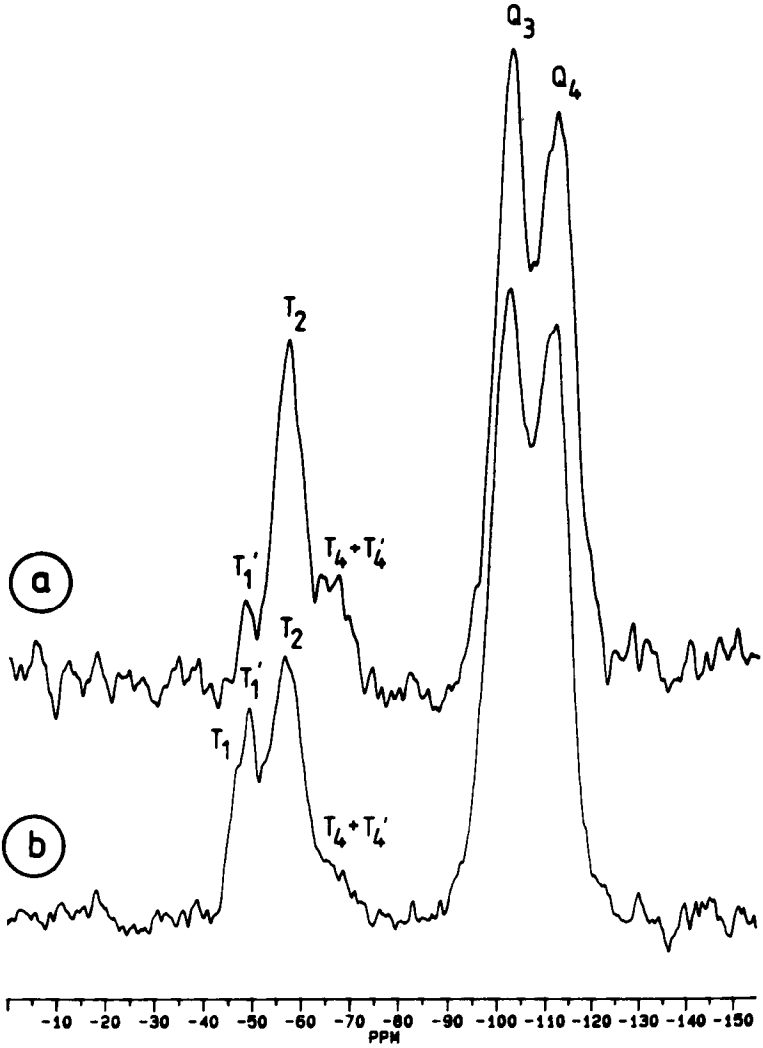

Fig. 11. ^{29}Si CP–MAS NMR spectrum of trifunctionally derivatized silica gel: (a) in the presence of air; (b) in an argon atmosphere.

trifunctionally, in contrast to difunctionally modified stationary phases, the amount of the monodentate species T_1 and T_1' is relatively low (Fig. 11). Their relative amounts, even for reactions in an argon atmosphere, do not exceed 10%. However, derivatization in an argon atmosphere mainly yields the bidentate species, T_2 (56%), and the cross-linked condensed species, $T_4 + T_4'$ (24%). Derivatization in air leads to a reduced amount of T_2 (26%), whereas the amount of the condensed species, $T_4 + T_4'$, increases to 65%.

In the case of trifunctional modification with trichlorosilane (Fig. 12), the reaction also starts with the formation of an intermediate, I, which can further react via

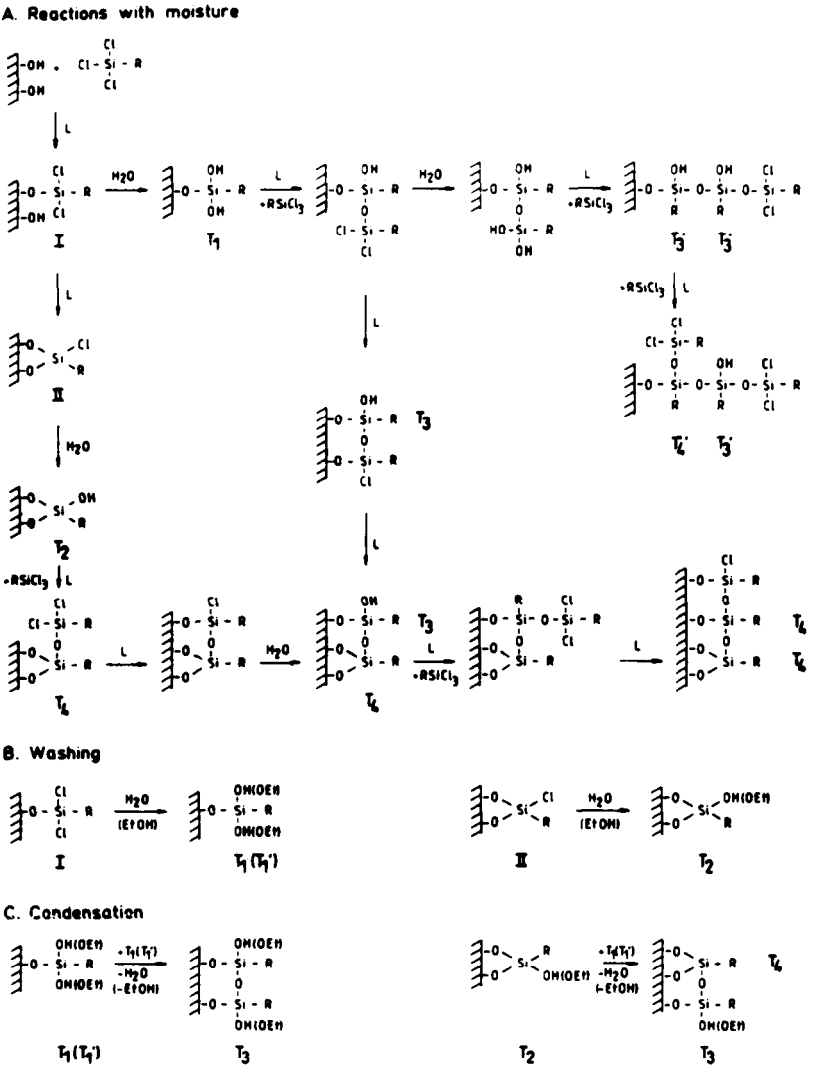

Fig. 12. Reaction scheme for trifunctional modification of silica gel.

two reaction pathways. One possibility is the reaction to bidentate II, which is hydrolyzed during washing to give bidentate T_2. The other possibility is the reaction with moisture to give T_1 and further formation of cross-links ($T_3 + T_3'$, $T_4 + T_4'$). The monodentate I is hydrolysed during washing to give monodentates T_1 and T_1'. In contrast to difunctional modification, the formation of II is obviously preferred, as only a small amount of T_1 and T_1' is obtained after washing the samples, whereas the amount of bidentate T_2 is very high. The species T_1', like the D_2 species, can only be formed during the washing step with ethanol, after the reaction procedure, and is therefore an indicator of the amount of intermediate I. Especially the derivatization in the presence of an argon atmosphere leads to an increase in bidentate species, T_2 (56%). The ratio of monodentate (T_1, T_1') to bidentate (T_2) is 1:7 in an argon atmosphere and 1:9 in the presence of moisture. The reason for the large amount of bidentate species may be that trichlorosilanes have three reactive groups, and hence higher probability of having the appropriate steric arrangement necessary for reaction with two neighbouring surface silanols, in contrast to dichlorosilanes with only two functional groups. The more moisture is available in the modification procedure, the more chlorine atoms of the trichlorosilanes are hydrolysed and therefore the formation of the T_2 species is reduced in favour of cross-linked species $T_3 + T_3'$ and $T_4 + T_4'$.

The concentration of the species polymerizing perpendicular to the surface (D_4', T_3' and T_4') seems to be relatively low, compared with the amounts of species polymerizing along the surface (D_4, T_3 and T_4), owing to steric hindrance of the bulky octadecyl chains. Therefore, condensation of monodentates yields mainly D_4, T_3 and T_4 species. Their amounts depend on the reaction procedure. Derivatization in the absence of an argon atmosphere causes increased condensation. The more moisture is available for the reaction, the more favoured is the competitive reaction of the monodentate I to D_1 or T_1 (Figs. 10 and 12), which can further react with chlorosilane, catalysed by 2,6-lutidine, to form the condensation products $D_4 + D_4'$ or T_3, T_3' and $T_4 + T_4'$. Hence the reduced amounts of D_2 or T_2 without an argon atmosphere are easily explained by assuming that most of the monodentate I has formed $D_4 + D_4'$ or $T_4 + T_4'$ before washing.

Condensation reactions seem to play a minor role in the modification procedure. This is indicated by the relatively small amount of D_3 or $T_3 + T_3'$ in all derivatized stationary phases.

4. INVESTIGATION OF END-CAPPING

The effect of end-capping with hexamethyldisilazane (HMDS) or trimethylchlorosilane (TMCS) can be seen in the ^{29}Si CP–MAS NMR spectra and in the ^{13}C CP–MAS NMR spectra. Fig. 13 shows the ^{29}Si CP–MAS NMR spectrum of a commercially available material. The strong resonance at +12 ppm in addition to the signals of T_1, T_2 and $T_4 + T_4'$ at −46 to −70 ppm indicates the introduction of a $Si(CH_3)_3$ moiety A to the silica surface. An additional resonance due to the $Si(CH_3)_3$ group can also be seen in the ^{13}C CP–MAS NMR spectrum (Fig. 14). Here, the increase in the signal at −1.3 ppm clearly shows the effect of end-capping the monofunctionally silylated silica gel.

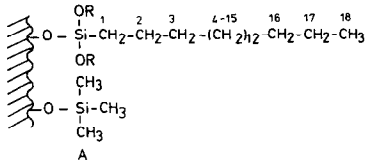

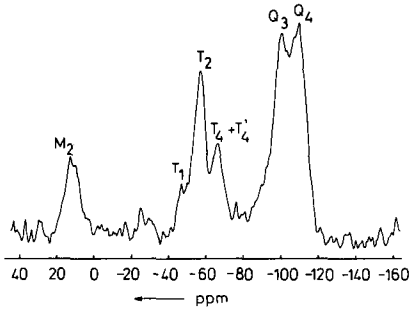

Fig. 13. ^{29}Si CP–MAS NMR spectrum of trifunctionally modified and end-capped material.

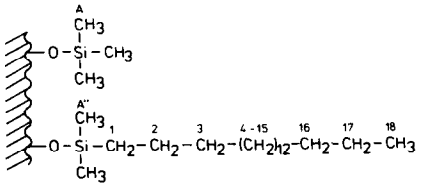

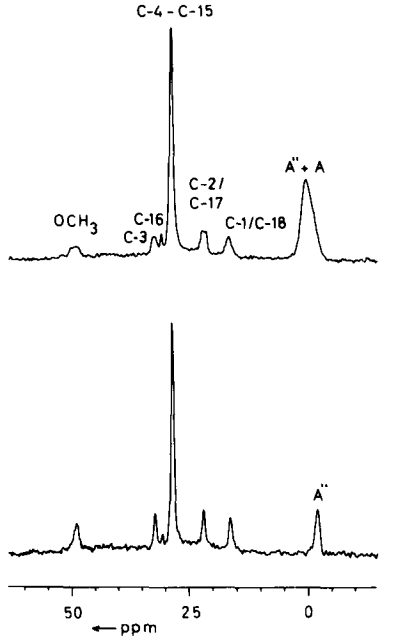

Fig. 14. ^{13}C CP–MAS NMR spectrum of monofunctionally modified and end-capped material.

5. INVESTIGATION OF AGEING EFFECTS

Changes in the selectivity and properties of reversed-phase (RP) packings are mainly caused by ageing effects. Information on structural changes on the bonded phases can be obtained if the RP phases are subjected to artificial ageing [30,32].

Artificial ageing experiments can be be performed by exposure of columns

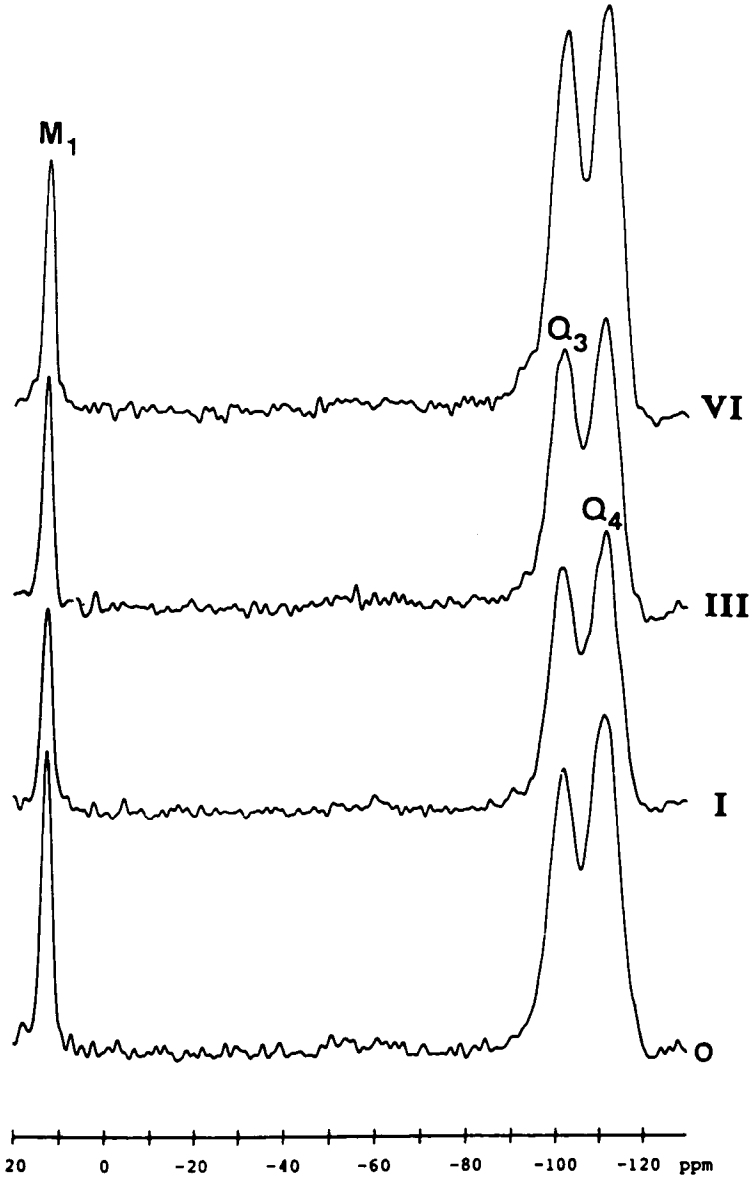

Fig. 15. ^{29}Si CP–MAS NMR spectra of monofunctionally modified silica gel, (0) before, and (I, III, VI; see text) after different treatments causing artificial ageing.

packed with investigated bonded phases to several eluent compositions for a period of 240 h. Basic (pH 8.4, I) and acidic (pH 3.0, IV) aqueous and methanol–aqueous buffer (0.5:99.5, II:V) [30] and acetonitrile [32] are used as flushing solvents. In order to study the effect of additional ionic species on bonded phases, 0.005 *M* triethylamine (VI) at high pH and 0.005 *M* hexylsulphonate (III) at low pH were added to the methanol–water buffers [30].

For monofunctionally modified stationary phases, a significant loss of signals is

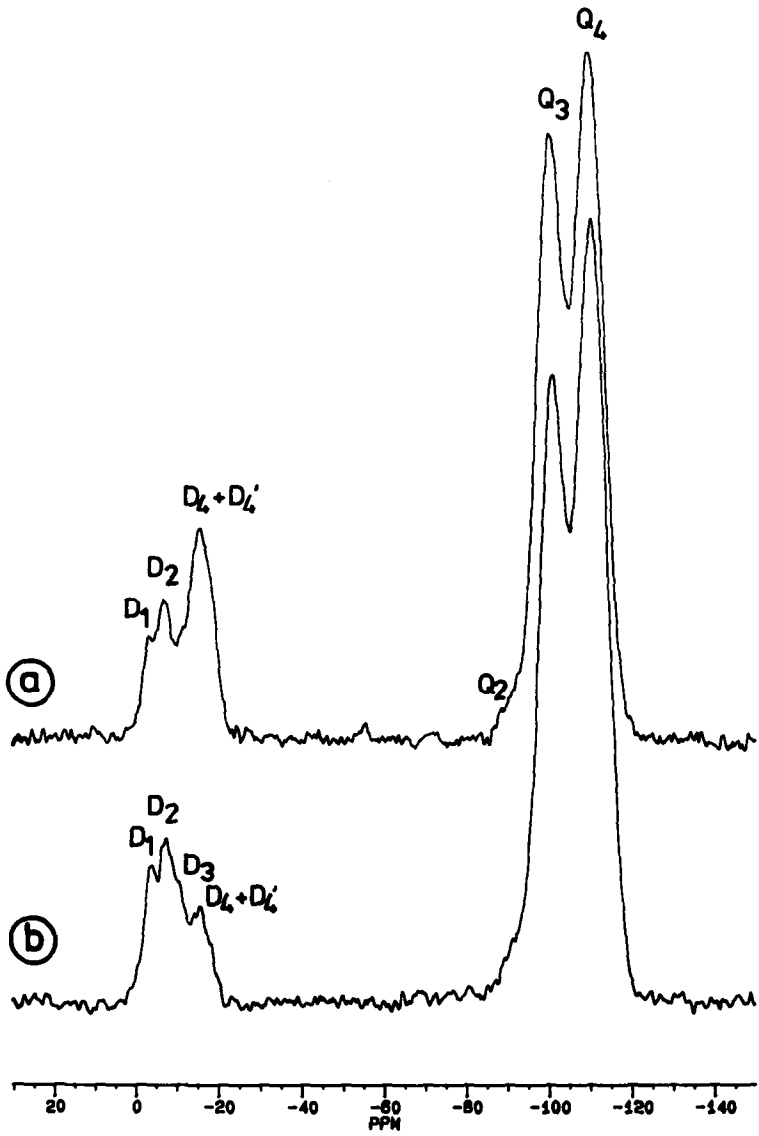

Fig. 16. ^{29}Si CP–MAS NMR spectra of difunctionally modified silica: (a) after and (b) before solvent exposure.

found. This is seen in Fig. 15, showing the ^{29}Si CP–MAS NMR spectra before (0) and after solvent exposure to aqueous acidic (I), methanol–aqueous acidic with acidic ion-paring agent hexylsulphonate (III) and methanol–aqueous basic with basic ion-pairing triethylamine eluent (VI) [30].

Flushing with acetonitrile causes a decrease in concentration of monodentate species D_1 and D_2 together with a significant increase in the concentration of the condensed species D_3 and $D_4 + D_4'$ in difunctionally derivatized silica gels [32]. As shown in Fig. 16, there is a 50% decrease in the amount of the monomeric species D_1 and D_2 (Fig. 16b), whereas the condensed species $D_4 + D_4'$ increase by 50% (Fig. 16a). Condensation, although slower, is also observed during ageing of dry stationary phases [32].

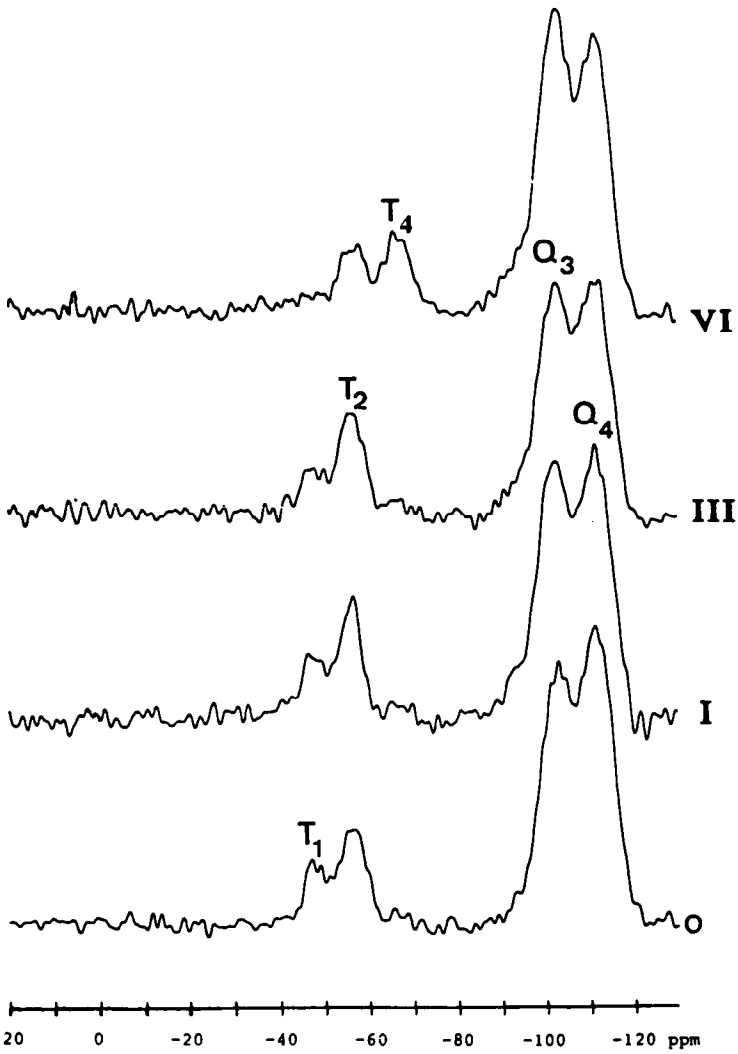

Fig. 17. ^{29}Si CP–MAS NMR spectra of trifunctionally modified silica gel, (0) before and (I, III, VI; see text) after different treatments causing artificial ageing.

The same phenomenon is observed when trifunctionally derivatized silica gel is flushed with aqueous acidic (I), methanol–aqueous acidic with acidic ion-pairing agent hexylsulphonate (III) and methanol–aqueous basic with basic ion-paring triethylamine eluent (VI) [30] (Fig. 17). The NMR spectra in Figs. 16 and 17 indicate that di- and trifunctional modified RP-HPLC phases tend to form more multidentate surface and neighbouring linkages of the octadecylsilane ligand when used intensively either with aqueous buffer solutions of high and low pH or with acetonitrile as eluents. Comparing the three types of modified silica gels, the multifunctional octadecylsilane stationary phases show a higher resistance towards ligand stripping.

6. ^{13}C CP–MAS NMR INVESTIGATIONS

The ^{13}C nucleus can be used in the investigation of bonded phases [33–37] in a similar way to the ^{29}Si nucleus, as ^{13}C nuclei, in contrast to ^{1}H nuclei, exhibit a chemical shift range of more than 200 ppm and dipolar broadening effects can be reduced by magic angle spinning. As a demonstration of the capability of ^{13}C CP–MAS NMR spectroscopy, the modification reaction of Nucleosil with octadimethylmethoxysilane is described by comparing the ^{13}C NMR spectra of the starting material and of the modified silica. The high-field region of the solution spectrum of octadecyldimethylmethoxysilane in benzene (Fig. 18) exhibits three different signals, which can be assigned to the $SiCH_3$ moiety A (-2.5 ppm), to the terminal methyl group C-18 (14.3 ppm) and the signal of C-1 (16.4 ppm). Further signals result from C-17 and C-2 at 22.3 and 22.8 ppm, respectively. The resonances of C-4 to C-15 are identical (30.2 ppm) because substitution effects of terminal groups such as CH_3, OH and SiR_3 are only active up to the γ-carbon atom. The signals of C-3 at 33.9 ppm and of C-16 at 32.3 ppm are shifted to lower field with respect to the strong resonance of C-4 to C-15. The ^{13}C solid-state NMR spectrum of the silica material chemically modified with octadimethylmethoxysilane shows all ^{13}C signals at similar chemical shifts (Fig. 19). The high resolution of solid-state NMR spectroscopy is also revealed

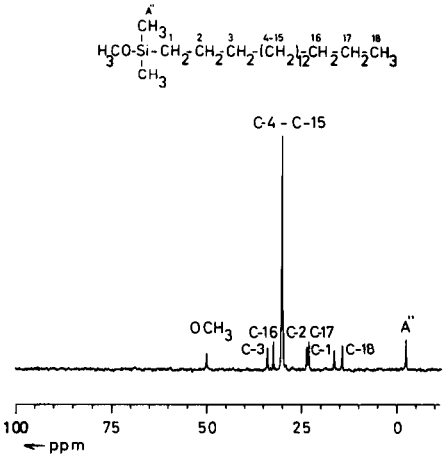

Fig. 18. Solution ^{13}C NMR spectrum of octadecyldimethylmethoxysilane in benzene-d_6.

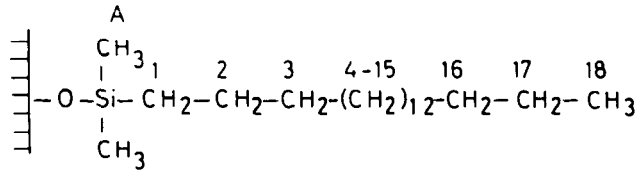

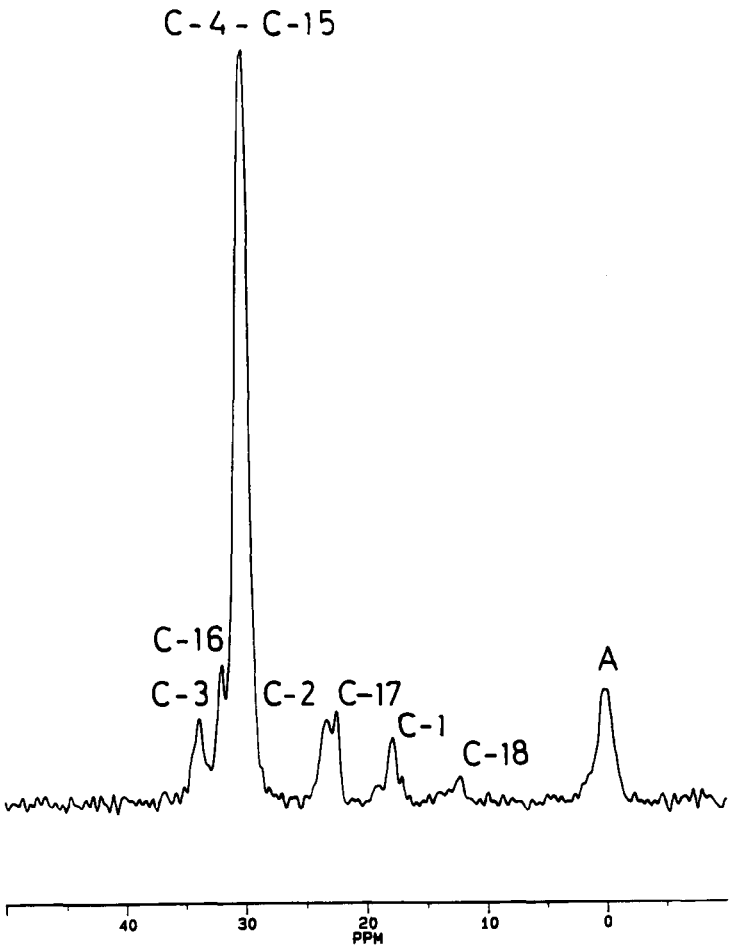

Fig. 19. ^{13}C CP–MAS NMR spectrum of the reaction product of silica gel and octadecyldimethylmethoxysilane.

by the ^{13}C CP–MAS NMR spectrum of a butyl phase (Fig. 20). Here, all resonances are resolved.

Structural changes of the attached alkylsilyl moiety caused by hydrolytic or protonating reactions are also revealed by ^{13}C CP–MAS NMR spectroscopy. Fig. 21 shows the ^{13}C NMR spectrum of silylglycidylpropyloxy-modified silica gel, indicat-

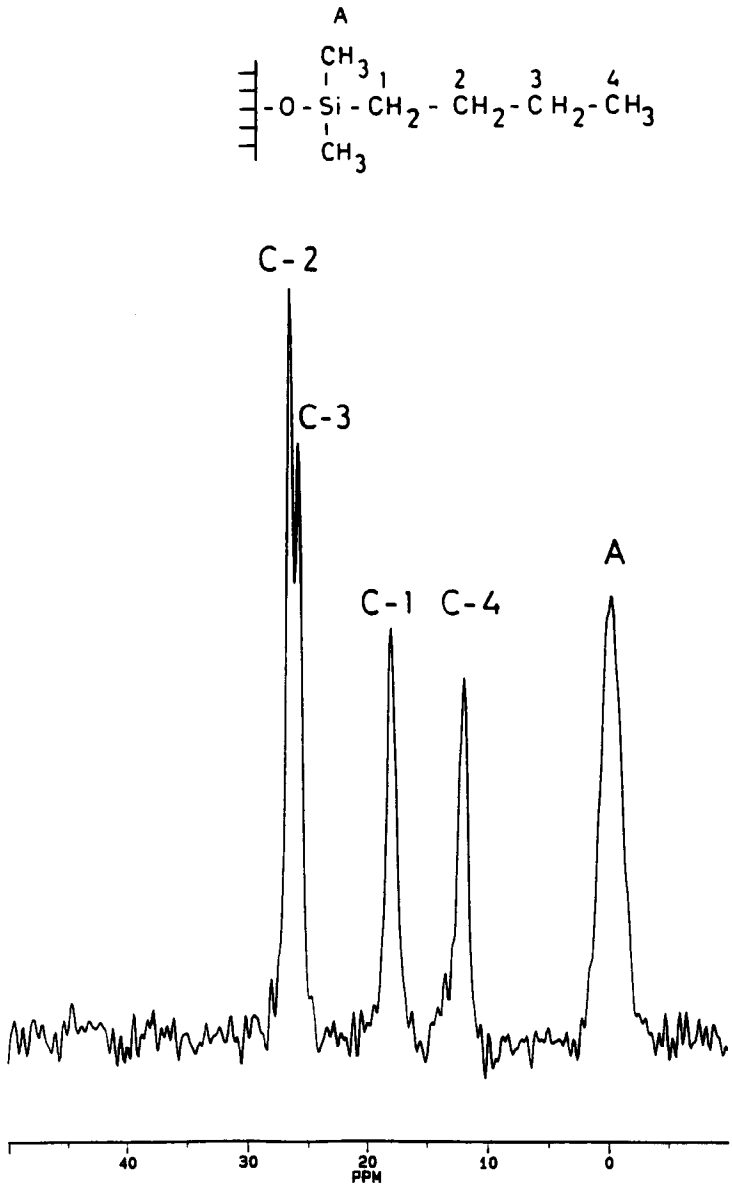

Fig. 20. ^{13}C CP–MAS NMR spectrum of the reaction product of silica gel and butyldimethylchlorosilane.

ing the different hydrolytic state of the oxirane moiety. The unhydrolysed compound is indicated by the oxirane signals C-5 (50.2 ppm) and C-6 (44.0 ppm). The hydrolysed ligand exhibits a new C-6′ signal of the dihydroxy moiety at 61.1 ppm (the dihydroxy C-5′ signal at 71.9 ppm cannot be resolved from the signals of C-3′, C-4′ and C-3–C-5). Owing to the different chemical shifts of the C-6 signal of the oxirane and the dihydroxy moieties, the amount of hydrolysis can be roughly estimated from

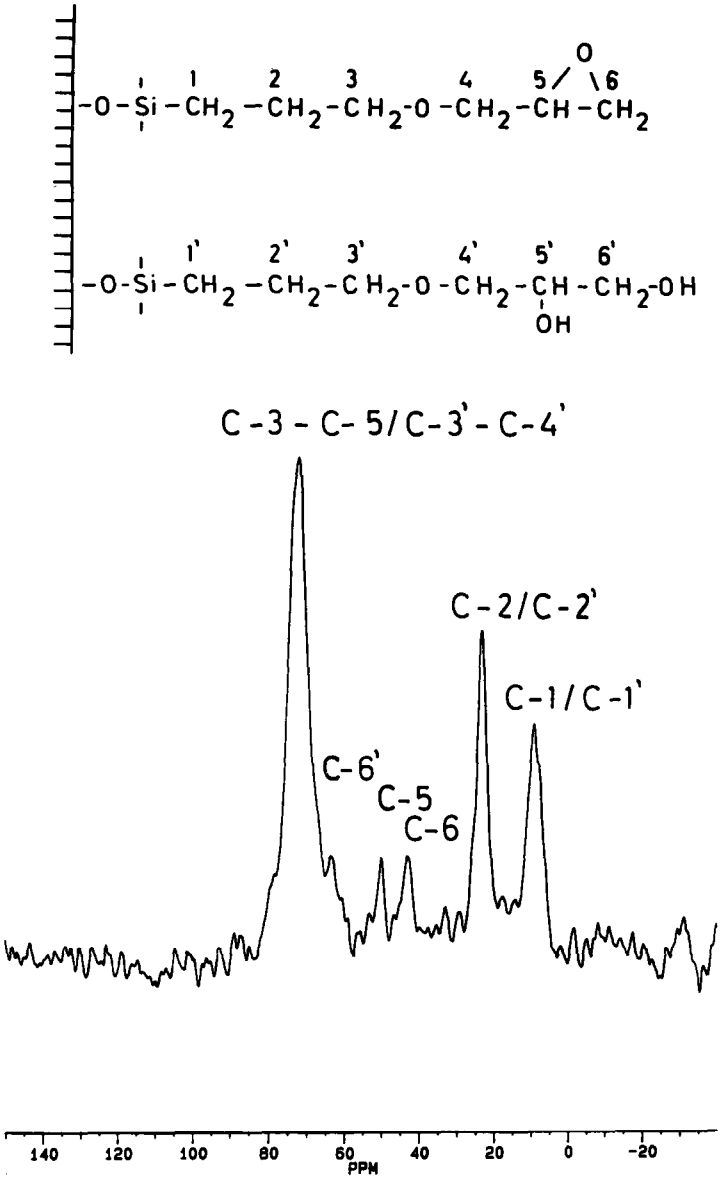

Fig. 21. ^{13}C CP–MAS NMR spectrum of silica gel silylated with glycidylpropyloxytriethoxysilane showing partial hydrolysis of the oxirane ring.

the ^{13}C CP–MAS NMR spectra. Fig. 21 shows that about half of the oxirane ring population has been hydrolysed to the dihydroxy compound.

In addition, ^{13}C chemical shifts give information about the coverage density. At high surface loads ($\geqslant 2.9$ μmol/m^2) two ^{13}C signals are found for the terminal methyl group of C_{18} phases [38]. The signal at 14.1 ppm can be attributed to a more rigid environment whereas the signal at 12.2 ppm is due to a carbon atom with greater

motional freedom. The existence of two distinct conformations of the terminal methyl group is only found in long alkyl chains ($n \geqslant 18$) and at high surface loads

The protonation state of a γ-aminopropyl-modified silica gel can be characterized by ^{13}C CP–MAS NMR spectroscopy. The free aminopropyl ligand is indicated by signals at 8.6 ppm (C-1), 26.2 ppm (C-2) and 41.8 ppm (C-3) [39]. In the protonated state, the signal of C-2 is shifted upfield to 16.8 ppm, whereas the signal of C-3 experiences a downfield shift to 52.8 ppm. Interestingly, both protonated and the unprotonated forms are found in silyl-γ-aminopropyl-modified silica prepared according to the procedure of Buszewski *et al.* [40].

7. STUDIES OF THE DYNAMIC BEHAVIOUR OF ALKYL-MODIFIED SILICA

The high resolution of ^{13}C solid-state NMR spectra (see Section 6) allows measurement of the dynamic behaviour of the carbon atoms via the resolved carbon signals of the alkyl chain without the necessity for labelling [37,41].

The motional behaviour of a distinct environment of the alkyl chain in the kHz range can be described by the ^{1}H and ^{13}C spin–lattice relaxation parameters in the rotating frame $T_{1\rho H}$ and $T_{1\rho C}$. Because $T_{1\rho C}$ values may be strongly influenced by spin–spin interactions [6] with resulting ambiguity of interpretation, only $T_{1\rho H}$ is available for probing spin dynamics.

In cross-linked polymers (*e.g.*, polystyrene), the $T_{1\rho H}$ values of different polymer carbons often appear as a single value as a result of spin diffusion caused by the rigid domain structure. In more flexible molecules, on the other hand, spin diffusion is quenched, as shown by Alemany *et al.* [42,43]. In the case of alkyl chains grafted to silica, different $T_{1\rho H}$ values are observed for each resolved carbon atom [36,37,41]. The dipolar interactions and thus spin diffusion are strongly reduced owing to the high motional freedom of the grafted alkyl chain in the solid state, combined with magic angle spinning at 4 kHz.

The dynamic behaviour of *n*-alkyl ligands with various *n*-alkyl chain lengths ($1 < n < 18$) was characterized by determination of $T_{1\rho H}$ [37,41]. Fig. 22 shows a typical set of ^{13}C CP–MAS NMR spectra obtained by the determination of the C_{12}-phase $T_{1\rho H}$. According to the length of the variable delay τ (indicated at the right-hand end of the spectrum), the ^{13}C signal intensity decreases. Comparing the signal intensities of C-2 and C-11 at $\tau = 6$ and 35 ms, the different $T_{1\rho H}$ behaviours of the protons associated with these carbon atoms are apparent. While it is evident that different $T_{1\rho H}$ values for the investigated high surface coverage RP materials are found, a straightforward interpretation of these different values is difficult. A great help in correlating higher and lower $T_{1\rho H}$ values with the appropriate correlation times in the 50-kHz motional regime is to observe the $T_{1\rho H}$ temperature dependence. Fig. 23 shows the $T_{1\rho H}$ values of the hexyl phase at five different temperatures. It can be seen that with increasing temperature, $T_{1\rho H}$ also increases, indicating that a decrease in the effective correlation time is correlated with longer $T_{1\rho H}$ times. Therefore, an increase in $T_{1\rho H}$ is connected with increasing mobility of the CH_2 group under consideration.

As also seen in Fig. 23, there is a continuous increase in $T_{1\rho H}$ values starting from the carbon anchored to the silica up to the carbon of the terminal methyl group. This finding can be explained by the increasing motional freedom within the alkyl chain with increasing distance from the silica surface.

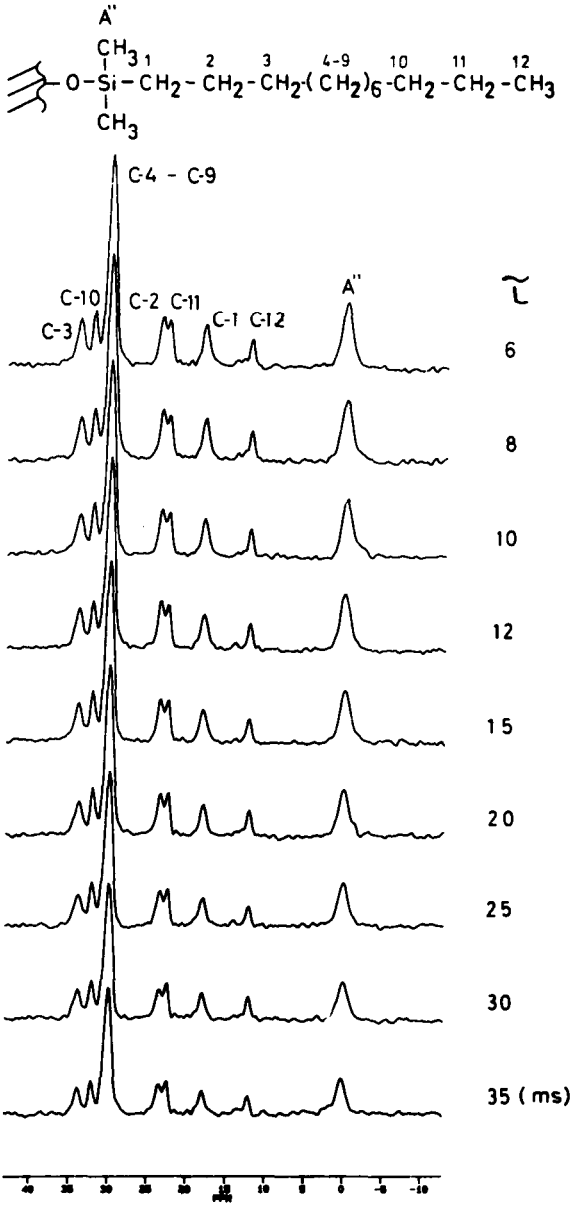

Fig. 22. $T_{1\rho H}$ determination for a C_{12} phase as a funtion of τ.

A systematic determination of $T_{1\rho H}$ values of various RP phases with similar surface coverages (3.5 μmol/m^2) reveals that highest values are observed with the C_6 phase and the C_8 phase (Fig. 24). Interestingly, the C_4 phase exhibits lower $T_{1\rho H}$ times han the C_{10} phase. Moreover, the smallest values are obtained with the C_{18} and C_{20} phases. According to these data, maximum mobility of the alkyl chain is attained with the C_6 and C_8 phases, whereas shorter and longer alkyl chains seem to exhibit less motional freedom.

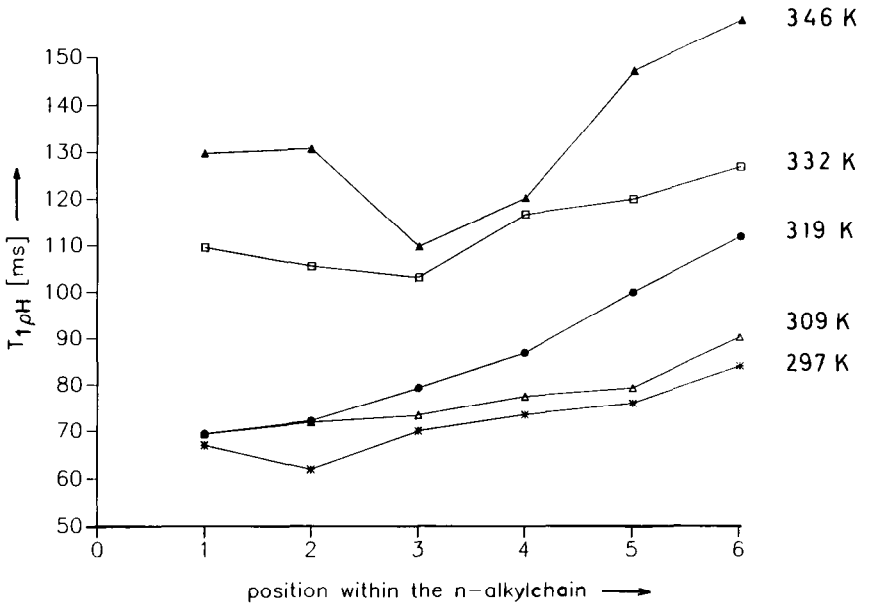

Fig. 23. Temperature-dependent $T_{1\rho H}$ measurements on a C_6 phase.

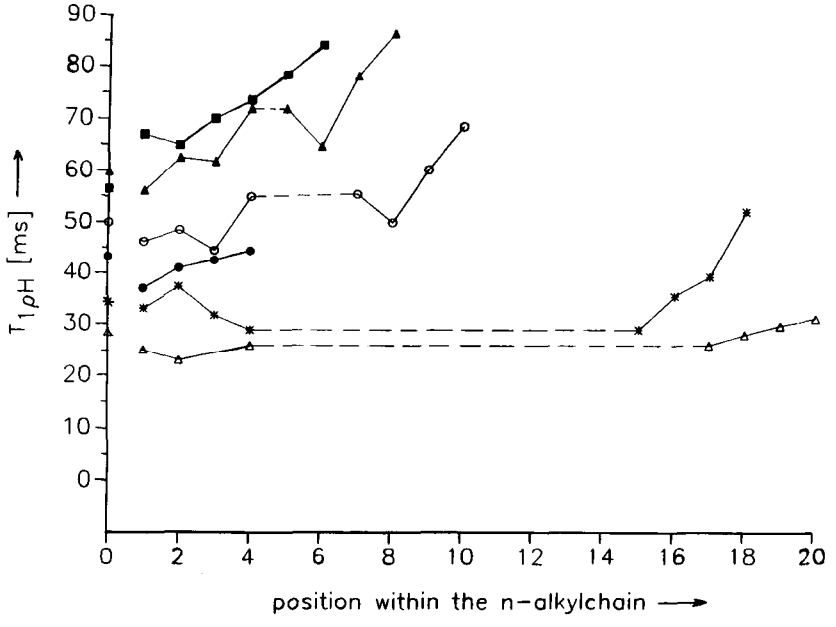

Fig. 24. Dependence of the $T_{1\rho H}$ values on the carbon position within the *n*-alkyl chain. *n* = (●) 4; (■) 6; (▲) 8; (○) 10; (✳) 18; (△) 20.

In monofunctionally derivatized silica gels with high surface coverage, the octyl alkyl chain exhibits the highest motional freedom. This phenomenon, already discussed by Berendsen and De Galan [44], is indicated by the described NMR relaxation parameters. This finding, however, is only valid for monolayers derived from dimethylalkylsilylsilica systems with high surface load and pore sizes of 100 Å; the dynamic behaviour of defined polymeric phases or of alkoxysilica systems may be totally different. Moreover the structure of the bulk support (*e.g.*, porous glass with different pore sizes or cross-linked polystyrene) may also lead to changes in the spin dynamics of the alkyl ligands.

These investigations show that the alkyl chains of bonded phases even in the solid state exhibit a liquid-like behaviour. The dynamic parameters obtained by solid-state NMR investigations are corroborated by suspended-state NMR spectroscopy [45–48].

In summary, ^{29}Si and ^{13}C CP–MAS NMR spectroscopy are extremely valuable tools for describing structural and dynamic features of bonded phases.

8. SYMBOLS

CP	Cross-polarization, transfer of proton spin polarization to ^{13}C (or ^{29}Si) spin polarization during a distinct contact time
CP curve	NMR signal amplitude behaviour as a function of the applied contact time
D_n	Surface species of difunctionally derivatized silica gel
H_{1H} (H_{1C}, H_{1Si})	Proton (^{13}C, ^{29}Si) radiofrequency field
MAS	Magic angle spinning
M_n	Surface species of monofunctionally derivatized silica gel
NMR	Nuclear magnetic resonance
Q_2	Geminal silanol groups
Q_3	Silanol groups
Q_4	Siloxane groups
Spin-lock condition	Transverse proton magnetization is maintained by H_{1H}
T_n	Surface species of trifunctionally derivatized silica gel
T_1	Spin–lattice relaxation time in the laboratory frame (MHz motional regime)
$T_{1\rho}$	Spin–lattice relaxation time in the rotating frame (kHz motional regime)
$T_{1\rho H}$	Proton spin–lattice relaxation time in the rotating frame, determines the decay of spin-locked proton magnetization and thus the fall-off of ^{13}C and ^{29}Si magnetization
T_{IS}(T_{CH}, T_{SiH})	Cross-relaxation constant, determines build-up of ^{13}C or ^{29}Si magnetization
γ	Gyromagnetic ratio

REFERENCES

1 K. K. Unger, *Porous Silica* (*Journal of Chromatography Library*, Vol. 16), Elsevier, New York, 1979.
2 L. C. Sanders and S. A. Wise, *CRC Crit. Rev. Anal. Chem.*, 18 (1987) 299.
3 J. Schaefer and E. O. Stejskal, *J. Am. Chem. Soc.*, 98 (1976) 1031.

4 J. Schaefer and E. O. Stejskal, *Top. Carbon NMR Spectrosc.*, 3 (1979) 283.
5 A. Pines, M. Gibby and J. S. Waugh, *Chem. Phys.*, 59 (1973) 569.
6 J. Schaefer, O. Stejskal and R. Buchdahl, *Macromolecules*, 10 (1977) 384.
7 G. Engelhardt, H. Janeke, E. Lippmaa and A. Samoson, *J. Organomet. Chem.*, 210 (1981) 295.
8 G. E. Maciel and D. W. Sindorf, *J. Am. Chem. Soc.*, 102 (1980) 7606.
9 B. Pfleiderer, K. Albert, E. Bayer, L. van de Ven, J. de Haan and C. Cramers, *J. Phys. Chem.*, 94 (1990) 4189.
10 M. Hetem, *Thesis*, Eindhoven University of Technology, 1990.
11 G. E. Berendsen and L. de Galan, *J. Liq. Chromatogr.*, 1 (1978) 561.
12 J. N. Kinkel and K. K. Unger, *J. Chromatogr.*, 316 (1984) 193.
13 H. Engelhardt, B. Dreyer and H. Schmidt, *Chromatographia*, 16 (1982) 11.
14 B. Buszewski, M. El Mouehli, K. Albert and E. Bayer, *J. Liq. Chromatogr.*, 13 (1990) 505.
15 D. W. Sindorf and G. E. Maciel, *J. Am. Chem. Soc.*, 105 (1981) 4263.
16 G. E. Maciel, D. W. Sindorf and V. J. Bartuska, *J. Chromatogr.*, 205 (1981) 438.
17 D. W. Sindorf and G. E. Maciel, *J. Phys. Chem.*, 86 (1982) 5208.
18 C.-H. Chiang, N. Liu and J. L. Koenig, *J. Colloid Interface Sci.*, 86 (1982) 26.
19 G. R. Hays, A. D. H. Claque, R. Huis and G. V. D. Velden, *Appl. Surf. Sci.*, 10 (1982) 247.
20 D. W. Sindorf and G. E. Maciel, *J. Am. Chem. Soc.*, 105 (1983) 1487.
21 E. Bayer, K. Albert, J. Reiners, M. Nieder and D. Müller, *J. Chromatogr.*, 264 (1983) 197.
22 H. A. Claessens, L. J. M. van de Ven, J. W. de Haan and C. A. Cramers, *J. High Resolut. Chromatogr. Chromatogr. Commun.*, 6 (1983) 433.
23 D. W. Sindorf and G. E. Maciel, *J. Am. Chem. Soc.*, 105 (1983) 3767.
24 D. W. Sindorf and G. E. Maciel, *J. Phys. Chem.*, 87 (1983) 5516.
25 L. Miller, R. W. Linton, G. E. Maciel and B. L. Hawkins, *J. Chromatogr.*, 319 (1985) 9.
26 L. J. M. van de Ven, J. G. Post, J. H. C. van Hooff and J. W. de Haan, *J. Chem. Soc., Chem. Commun.*, (1985) 214.
27 J. W. de Haan and L. van de Ven, *J. Colloid Interface Sci.*, 110 (1986) 591.
28 K. Albert, B. Pfleiderer and E. Bayer, in D. E. Leyden and W. T. Collins (Editors), *Chemically Modified Surfaces*, Vol. 2, Gordon and Breach, New York, 1988, p. 287.
29 J. M. J. Vankan, J. J. Ponjee, J. W. de Haan and L. J. M. van de Ven, *J. Colloid Interface Sci.*, 126 (1988) 604.
30 M. Hetem, L. van de Ven, J. de Haan, C. Cramers, K. Albert and E. Bayer, *J. Chromatogr.*, 479 (1989) 269.
31 B. Buszewski, *Chromatographia*, 29 (1990) 233.
32 B. Pfleiderer, K. Albert and E. Bayer, *J. Chromatogr.*, 506 (1990) 343.
33 D. E. Leyden, D. S. Kendall, L. Burggraf, F. J. Pern and M. DeBellow, *Anal. Chem.*, 54 (1982) 101.
34 D. W. Sindorf and G. E. Maciel, *J. Am. Chem. Soc.*, 105 (1983) 1848.
35 G. E. Maciel, R. C. Zeigler and R. K. Taft, in D. E. Leyden and W. T. Collin (Editors), *Chemically Modified Surfaces*, Vol. 1, Gordon and Breach, New York, 1986, p. 413.
36 R. C. Zeigler and G. E. Maciel, in D. E. Leyden and W. T. Collins (Editors), *Chemically Modified Surfaces*, Vol. 2, Gordon and Breach, New York, 1988, p. 319.
37 K. Albert, B. Pfleiderer and E. Bayer, in D. E. Leyden, W. T. Collins and C. H. Lochmüller (Editors), *Chemically Modified Surfaces*, Vol. 3, Gordon and Breach, New York, 1990, p. 233.
38 B. Pfleiderer, *Thesis*, Eberhard Karls University, Tübingen, 1989.
39 C. S. Caravajal, D. E. Leyden, G. R. Quinting and G. E. Maciel, *Anal. Chem.*, 60 (1986) 1776.
40 B. Buszewski, J. Schmid, K. Albert and E. Bayer, *J. Chromatogr.*, in press.
41 B. Pfleiderer, K. Albert, K. D. Lork, K. K. Unger, H. Brückner and E. Bayer, *Angew. Chem., Int. Ed. Engl.*, 28 (1989) 327.
42 L. B. Alemany, D. B. Grant, E. J. Pugmire, T. D. Alger and K. W. Zilm, *J. Am. Chem. Soc.*, 105 (1983) 2133.
43 L. B. Alemany, D. B. Grant, R. J. Pugmire, T. D. Alger and K. W. Zilm, *J. Am. Chem. Soc.*, 105 (1983) 2142.
44 G. E. Berendsen and L. de Galan, *J. Chromatogr.*, 196 (1980) 21.
45 K. Tanaka, S. Shinoda and Y. Saito, *Chem. Lett.*, (1970) 179.
46 K. Albert, B. Evers and E. Bayer, *J. Magn. Reson.*, 62 (1985) 428.
47 R. K. Gilpin, *Anal. Chem.*, 57 (1985) 1465A, and references cited therein.
48 E. Bayer, A. Paulus, B. Peters, G. Laupp, J. Reiners and K. Albert, *J. Chromatogr.*, 364 (1986) 25.